# Formulation of a Novel Implicit Stress Integration Algorithm based on Plastic Consistency Parameter and its Verification Using von Mises Plasticity

*M. A. K. M. Dharmasiri[1], †Maddegedara Lalith[2], Kohei Fujita[2], Tsuyoshi Ichimura[2] and Muneo Hori[3]

[1]Dept. of Civil Eng., The Univ. of Tokyo, Japan
[2]Earthquake Research Inst., The Univ. of Tokyo, Japan
[3]Japan Agency for Marine-Earth Science and Technology, Yokohama, Japan
*Presenting author: kasun@eri.u-tokyo.ac.jp
†Corresponding author: lalith@eri.u-tokyo.ac.jp

## Abstract

We propose a novel algorithm for integrating the standard rate form of plasticity in which the state variables are gradually returned onto the yield surface by a series of implicit plastic correction stages. Its features are discussed in relation to the Closest Point Projection Method (CPPM) and the Cutting Plane Method (CPM). As in CPPM, it is straightforward to derive a consistent tangent operator for the proposed method. Like in CPM, it uses the successive linearization of the yield function about the current state to evaluate the state variables. The proposed integration method can be easily implemented in existing finite element analysis frameworks since the required first and second order derivatives are similar to those required in CPPM. Several numerical tests are performed using von Mises plasticity and linear hardening rules. Single material point tests reveal that the proposed algorithm provides near identical stress remapping to that of CPM and CPPM. For the classical perforated sheet benchmark with both linear isotropic hardening and linear kinematic hardening, CPM, CPPM and the proposed methods produce near identical results. For the combined hardening, a slight disparity between the results from CPPM with the other two methods is observed. Further, the multi-element tests demonstrate that the consistent tangent operator of the proposed method is on par with that of CPPM.

**Keywords:** plasticity; integrating the rate form; consistent tangent operator; von Mises;

## 1 Introduction

Recent advances in computing has made large scale simulations involving nonlinear analysis a reality. Search for novel algorithms for nonlinear problems can contribute to optimally utilizing the available computational resources by choosing suitable algorithm according to the simulated phenomena and the computer hardware. One such nonlinear problem is classical plasticity. Dependig on the required accuracy, involved phenomena, stability, parallel computing model, etc. we can choose a suitable algorithm for integrating the rate-form of classical plasticity from a number of algorithms available. Scalet and Auricchio [1] provides an excellent summary of such classical and less classical methods used for stress integration.

Closest Point Projection Method (CPPM)[2] and the Cutting Plane Method (CPM)[3] are the most popular classical algorithms used to predict the evolution of state variables such as stresses and plastic internal variables. The earliest ideas about CPPM were set forth by Wilkins [2] and subsequent contributions by several others have made this implicit algorithm, a very capable, accurate, albeit a relatively computationally costly numerical integration scheme. The CPM on the other hand, which was introduced by Ortiz and Simo [3], is an incomplete implicit algorithm which follows the path of the steepest descent [4] to arrive at estimates for the state variables during plastic deformations. Summarily, it could be said that for state variable remapping, CPPM is computationally costly due to its reliance on the second order derivatives for stress integration procedure, and CPM, in this regard, is computationally inexpensive. CPPM uses a residual based approach to estimate the remapped stresses while CPM utilizes successive linearization of the yield functions at the current state to estimate the plastic consistency parameter, thereby updating the state variables.Though computationally expensive CPPM is unconditionally stable, while computationally light CPM is not.

In this study, having observed these classical methods, an attempt has been made to introduce an implicit numerical integration scheme for rate independent plasticity, in which the state variables are gradually returned onto the yield surface by a series of implicit plastic correction stages. Similar to CPM, in the proposed method, the state variables are evaluated by the successive linearization of the yield function about the current state. For state variables remapping, the proposed scheme also require second order derivatives, like in CPPM. However, the solution strategy is marginally lower in terms of computational cost to that of CPPM, per iteration basis, for state variables remapping excluding the evaluation of the consistent tangent operator. On the other hand, the proposed framework requires iterative update of elasto-plastic tangent operator during material point iterations unlike in CPPM, which is evaluated only once during material point iterations. However, the overall computational efficiency depends not only on the computational cost for each of the material point iterations, but also on the accuracy of the elasto-plastic tangent operator and how accurate a prediction can be made regarding the evolution of state variables during material point iterations.

A brief summary of the classical theory of plasticity [5, 6] which is the basis for all of the three stress integration algorithms, CPPM, CPM and the proposed method is presented in section 2. The stress integration algorithms and the elasto-plastic tangent operators of CPPM, CPM and the proposed method and a comparison of their features is presented in section 3. In this paper, von Misses plasticity is used to study the accuracy and the performance of the newly minted proposed stress integration algorithm with its consistent tangent operator, in relation to CPPM and CPM methods. The verification problems considered and the results with a comparison are presented in section 4.

We use $\dot{f}$ to denote the time derivative of the quantity $f$ and when quantities are represented with two superscripts separated by a comma, i.e. $(.)^{p,k}$, the first superscript $p$ denotes the state whereas the second superscript $k$ denotes the material point iteration.

## 2 Classical Flow Theory of Plasticity

We consider classical flow theory [5, 6] based rate independent infinitesimal elasto-plastic deformations of an isotropic continuum subjected to suitable Dirichlet and Neumann boundary conditions prescribed as a function of time $t \in \mathbb{R}^+$. The linearized Green strain tensor for the induced infinitesimal deformation field $\boldsymbol{u}$ is defined as

$$\boldsymbol{\varepsilon} = \nabla^{sym}\boldsymbol{u} \tag{2.1}$$

Following Coleman [7], the history dependence of stress is quantified as

$$\boldsymbol{\sigma} = \boldsymbol{\sigma}\left(\boldsymbol{\varepsilon}, \boldsymbol{\kappa}\right), \tag{2.2}$$

where the internal plastic variable $\boldsymbol{\kappa}$ consists of hardening parameters such as the size of the yield surface (isotropic hardening) and translation direction of the yield surface (back stress in kinematic hardening). Further, we assume that that following assumptions of the classical plasticity theory hold true.

1. Additive decomposition $\boldsymbol{\varepsilon} = \boldsymbol{\varepsilon}^e + \boldsymbol{\varepsilon}^p$, where $\boldsymbol{\varepsilon}^e$ and $\boldsymbol{\varepsilon}^p$ are elastic and plastic contributions.

2. $\boldsymbol{\sigma} = \mathbf{C} : \boldsymbol{\varepsilon}^e$, where $\mathbf{C}$ is the fourth order elastic tangent tensor. This implies

$$\dot{\boldsymbol{\sigma}} = \mathbf{C} : (\dot{\boldsymbol{\varepsilon}} - \dot{\boldsymbol{\varepsilon}}^p)\,. \tag{2.3}$$

3. The stress should always satisfy $\phi\left(\boldsymbol{\sigma}, \boldsymbol{\kappa}\right) \leq 0$, where $\phi\left(\boldsymbol{\sigma}, \boldsymbol{\kappa}\right)$ is a suitable convex scalar function known as the yield criterion. Material behaves elastically when $\phi\left(\boldsymbol{\sigma}, \boldsymbol{\kappa}\right) < 0$ and plastically when $\phi\left(\boldsymbol{\sigma}, \boldsymbol{\kappa}\right) = 0$.

4. The evolution of $\dot{\boldsymbol{\varepsilon}}^p$ and $\dot{\boldsymbol{\kappa}}$ are defined by

$$\begin{aligned} \dot{\boldsymbol{\varepsilon}}^p &= \dot{\lambda}\boldsymbol{m} \\ \dot{\boldsymbol{\kappa}} &= \dot{\lambda}\mathbf{A}(\boldsymbol{\sigma}, \boldsymbol{\kappa}, \boldsymbol{\varepsilon}^p) \end{aligned} \tag{2.4}$$

   where $\dot{\lambda}\,(\geq 0)$ is the plastic consistency parameter, $\boldsymbol{m} = \frac{\partial\psi}{\partial\boldsymbol{\sigma}}$ is the flow vector specifying the direction of the plastic flow (where $\psi$ is the plastic potential surface and for associative flow rules $\psi = \phi$), and $\mathbf{A}(\boldsymbol{\sigma}, \boldsymbol{\kappa}, \boldsymbol{\varepsilon}^p)$ is the generalized form of hardening modulus. Furthermore, we can impose the consistency condition that $\dot{\lambda}\dot{\phi} = 0$ and Kuhn–Tucker complementary conditions that $\dot{\lambda} \geq 0, \quad \phi \leq 0, \quad \dot{\lambda}\phi = 0$ on the consistency parameter, $\dot{\lambda}$ and yield criterion, $\phi$.

## 3 Stress Integration Algorithms and Elasto-plastic Tangent Operators

Due to their non-linear nature, numerical schemes are required to integrate the governing rate forms of plasticity given by the Eqs. 2.3, and 2.4. Most of the available numerical methods make different approximations for these rate forms to obtain numerical schemes with different properties. In this section, we present the formulations of the widely used CPM and CPPM, and a novel fully implicit return mapping stress integration algorithm in which the state variables are gradually returned onto the yield surface by a series of implicit plastic correction stages.

For nonlinear finite element analysis using Newton-Raphson method, a material tangent operator is required to compute the element stiffness matrix. There are two tangent operators, such as the continuum tangent operator and the consistent tangent operator. The continuum tangent operator is constructed by making use of the satisfaction of the plastic consistency condition stated in section 2, while the consistent tangent operator is consistent with the algorithm that is used to compute the state variables. While the continuum tangent operator can be used as the elastoplastic tangent modulus / operator in any numerical integration scheme, the consistent tangent operator may not be available for some integration schemes. In this study, we also present the formulation of a consistent tangent operator for the proposed algorithm. .

The non-linear nature of plastic deformation problems requires two levels of iterative solving using suitable numerical schemes; global-level iterations using a scheme such as Newton-Raphson to determine displacement field of the domain, and material-level iterations to determine the resulting state of stress using a scheme such as CPPM. In the following discussion, we assume that we are at the $(k+1)^{th}$ material-level iteration of the $(n+1)^{th}$ load step (global-level iteration).

### *3.1 Cutting Plane Method (CPM)*

The main characteristic of CPM is that it express all the state variable as a function of the plastic consistency parameter $\Delta\lambda$ (i.e., $\boldsymbol{\sigma} = \boldsymbol{\sigma}(\Delta\lambda)$ and $\boldsymbol{\kappa} = \boldsymbol{\kappa}(\Delta\lambda)$) and linearizes $\phi$ with respect to $\Delta\lambda$ around the current state (i.e. $\boldsymbol{\sigma}^k$ and $\boldsymbol{\kappa}^k$).

CPM approximates $\boldsymbol{\sigma}^{k+1}$ and $\boldsymbol{\kappa}^{k+1}$ as

$$
\begin{aligned}
\boldsymbol{\sigma}^{k+1} &= \begin{cases} \boldsymbol{\sigma}_e = \boldsymbol{\sigma}_n + \mathbf{C} : \boldsymbol{\Delta\varepsilon} & \text{if } k = 0 \\ \boldsymbol{\sigma}^k - \Delta\lambda \mathbf{C} : \boldsymbol{m}^k & \text{if } k > 0 \end{cases} \\
\boldsymbol{\kappa}^{k+1} &= \begin{cases} \boldsymbol{\kappa}_n & \text{if } k = 0 \\ \boldsymbol{\kappa}^k + \frac{\partial \boldsymbol{\kappa}}{\partial \Delta\lambda}\Big|^k \delta\lambda & \text{if } k > 0, \end{cases}
\end{aligned} \tag{3.1}
$$

and expresses $\phi$ as a function of state variables at unknown state as $\phi\left(\boldsymbol{\sigma}^{k+1}(\Delta\lambda), \boldsymbol{\kappa}^{k+1}(\Delta\lambda)\right) = 0$. To iteratively solve this nonlinear function, CPM linearizes $\phi^{k+1}$ around the the current state $\left(\boldsymbol{\sigma}^k, \boldsymbol{\kappa}^k\right)$ as

$$
\phi^{k+1} \approx \phi^k + \left( \frac{\partial \phi}{\partial \boldsymbol{\sigma}}\bigg|^k : \frac{\partial \boldsymbol{\sigma}}{\partial \Delta\lambda}\bigg|^k + \frac{\partial \phi}{\partial \boldsymbol{\kappa}}\bigg|^k : \frac{\partial \boldsymbol{\kappa}}{\partial \Delta\lambda}\bigg|^k \right) \delta\lambda = 0. \tag{3.2}
$$

Accordingly, $\delta\lambda$ is determined as

$$
\delta\lambda = \left[ \frac{\partial \phi}{\partial \boldsymbol{\sigma}}\bigg|^k : \mathbf{C} : \boldsymbol{m}^k - \frac{\partial \phi}{\partial \boldsymbol{\kappa}}\bigg|^k : \frac{\partial \boldsymbol{\kappa}}{\partial \Delta\lambda}\bigg|^k \right]^{-1} \phi^k \tag{3.3}
$$

and the state variables are updated as

$$
\begin{aligned}
\boldsymbol{\sigma}^{k+1} &= \boldsymbol{\sigma}^k + \frac{\partial \boldsymbol{\sigma}}{\partial \Delta\lambda}\bigg|^k \delta\lambda \\
\boldsymbol{\kappa}^{k+1} &= \boldsymbol{\kappa}^k + \frac{\partial \boldsymbol{\kappa}}{\partial \Delta\lambda}\bigg|^k \delta\lambda.
\end{aligned} \tag{3.4}
$$

The above two steps are repeated until a suitable convergence criteria are met. Figure 3.1a depicts the stress return (mapping) during local (material level) iterations when CPM is used for numerical integration.

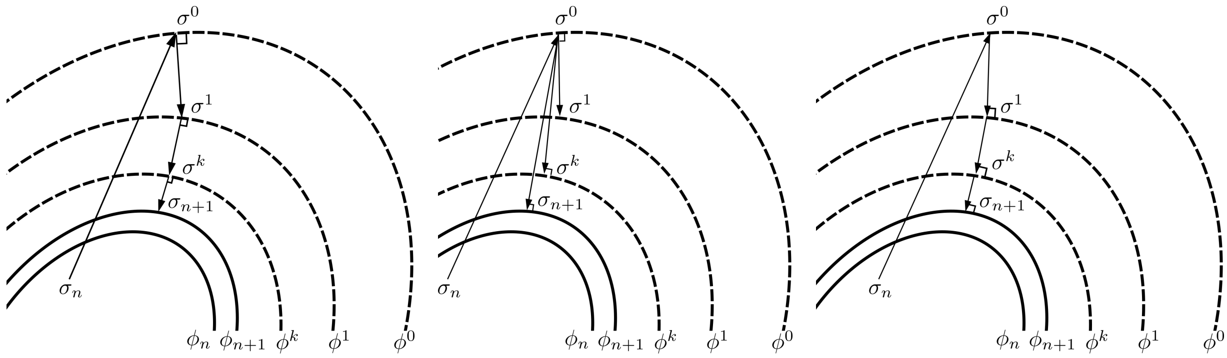


(a) CPM (b) CPPM (c) Proposed algorithm

**Figure 3.1: Stress return mapping during CPM, CPPM and the numerical integration**

The continuum tangent operator, which is generally used with CPM [4], is given by,

$$\mathbf{C}^{ep} = \mathbf{C} - \frac{(\mathbf{C} : \boldsymbol{m}) \otimes (\boldsymbol{n} : \mathbf{C})}{\boldsymbol{n} : \mathbf{C} : \boldsymbol{m} + \mathrm{K}^{\mathrm{p}}}, \tag{3.5}$$

where $\boldsymbol{n} = \frac{\partial \phi}{\partial \boldsymbol{\sigma}}$ and $\mathrm{K}^{\mathrm{p}} = -\frac{\partial \phi}{\partial \boldsymbol{\kappa}} : \frac{\partial \boldsymbol{\kappa}}{\partial \Delta\lambda}$. A consistent tangent operator was introduced later to CPM by Starmen et al. [8] which is not considered in this paper.

### *3.2 Closest Point Projection Method (CPPM)*

The earliest ideas pertaining to CPPM were suggested by Wilkins [2] for von Misses plasticity. Since then, various extensions such as application to linear isotropic and kinematic hardening [9], nonlinear hardening [10] have been added to CPPM. CPPM is well reputed for its accuracy, robustness and stability [4]. In contrast to CPM, CPPM regards the $\boldsymbol{\sigma}$, $\boldsymbol{\kappa}$ and $\Delta\lambda$ as independent variables.

CPPM is based on the following approximations for the rate forms given by Eqs. 2.3, and 2.4.

$$\begin{aligned}
\boldsymbol{\sigma}^{k+1} &= \begin{cases} \boldsymbol{\sigma}_e = \boldsymbol{\sigma}_n + \mathbf{C} : \boldsymbol{\Delta\varepsilon} & \text{if } k = 0 \\ \boldsymbol{\sigma}_e - \Delta\lambda^{k+1}\mathbf{C} : \boldsymbol{m}^{k+1} & \text{if } k > 0 \end{cases} \\
\boldsymbol{\kappa}^{k+1} &= \begin{cases} \boldsymbol{\kappa}_n & \text{if } k = 0 \\ \boldsymbol{\kappa}_n + \mathbf{A}\left(\boldsymbol{\sigma}^{k+1}, \boldsymbol{\kappa}^{k+1}, \Delta\lambda^{k+1}\right) & \text{if } k > 0 \end{cases}
\end{aligned} \tag{3.6}$$

The above expressions are nonlinear since the right hand sides are expressed in terms of the unknown state variables $\boldsymbol{\sigma}^{k+1}$, $\boldsymbol{\kappa}^{k+1}$ and $\Delta\lambda^{k+1}$. CPPM obtains an iterative scheme to solve these nonlinear equations based on the following residuals.

$$\begin{aligned}
\mathbf{r}_{\boldsymbol{\sigma}}^{k+1} &= \boldsymbol{\sigma}^{k+1} - \left[\boldsymbol{\sigma}_e - \Delta\lambda^{k+1}\mathbf{C} : \boldsymbol{m}^{k+1}\right] \\
\boldsymbol{r_\kappa}^{k+1} &= \boldsymbol{\kappa}^{k+1} - \left[\boldsymbol{\kappa}_n + \mathbf{A}\left(\boldsymbol{\sigma}^{k+1}, \boldsymbol{\kappa}^{k+1}, \Delta\lambda^{k+1}\right)\right] \\
r_\phi^{k+1} &= \phi\left(\boldsymbol{\sigma}^{k+1}, \boldsymbol{\kappa}^{k+1}, \Delta\lambda^{k+1}\right)
\end{aligned} \tag{3.7}$$

Taking Taylor expansion about the solution at $k^{th}$ iteration, ignoring higher order terms, and setting the residuals $\mathbf{r}_{(.)}\left(\boldsymbol{\sigma}^{k+1}, \boldsymbol{\kappa}^{k+1}, \Delta\lambda^{k+1}\right) = \mathbf{0}$, we can obtain the following linear set of equations for $\boldsymbol{\delta\sigma}$, $\boldsymbol{\delta\kappa}$, and $\delta\lambda$, which are the incremental updates of $\boldsymbol{\sigma}$, $\boldsymbol{\kappa}$, and $\Delta\lambda$, respectively.

Note that we drop the superscripts and subscripts for convenience, and all the terms in the right hand sides are evaluated at the solution of $k^{th}$ iteration. Here, $\mathbf{I}^{sym}$ is the fourth order major symmetric identity tensor.

$$\left\{ \begin{array}{c} \boldsymbol{\delta\sigma} \\ \boldsymbol{\delta\kappa} \\ \delta\lambda \end{array} \right\} = - \left[ \begin{array}{ccc} \mathbf{I}^{sym} + \Delta\lambda \mathbf{C} : \frac{\partial \boldsymbol{m}}{\partial \boldsymbol{\sigma}} & \Delta\lambda \mathbf{C} : \frac{\partial \boldsymbol{m}}{\partial \boldsymbol{\kappa}} & \mathbf{C} : \boldsymbol{m} \\ -\frac{\partial \mathbf{A}}{\partial \boldsymbol{\sigma}} & \mathbf{I}^{sym} - \frac{\partial \mathbf{A}}{\partial \boldsymbol{\kappa}} & -\frac{\partial \mathbf{A}}{\partial \Delta\lambda} \\ \frac{\partial \phi}{\partial \boldsymbol{\sigma}} & \frac{\partial \phi}{\partial \boldsymbol{\kappa}} & 0 \end{array} \right]^{-1} \left\{ \begin{array}{c} \mathbf{r}^k_{\boldsymbol{\sigma}} \\ \mathbf{r}^k_{\boldsymbol{\kappa}} \\ r^k_{\phi} \end{array} \right\} \tag{3.8}$$

Solving the above, we can incrementally update the state variables $\boldsymbol{\sigma}^{k+1}$, $\boldsymbol{\kappa}^{k+1}$ and $\Delta\lambda^{k+1}$ as follows until requisite convergence criteria are met. Figure 3.1b depicts how the stress is updated by the CPPM's return mapping iterations.

$$\begin{aligned} \boldsymbol{\sigma}^{k+1} &= \boldsymbol{\sigma}^k + \boldsymbol{\delta\sigma} \\ \boldsymbol{\kappa}^{k+1} &= \boldsymbol{\kappa}^k + \boldsymbol{\delta\kappa} \\ \Delta\lambda^{k+1} &= \Delta\lambda^k + \delta\lambda \end{aligned} \tag{3.9}$$

Differentiating Eq. (3.6) and the yield criterion with respect to $\boldsymbol{\Delta\varepsilon}$, we can obtain

$$\left[ \begin{array}{c} \frac{\partial \sigma}{\partial \boldsymbol{\Delta\varepsilon}} \\ \frac{\partial \kappa}{\partial \boldsymbol{\Delta\varepsilon}} \\ \frac{\partial \Delta\lambda}{\partial \boldsymbol{\Delta\varepsilon}} \end{array} \right] = \left[ \begin{array}{ccc} \mathbf{I}^{sym} + \Delta\lambda \mathbf{C} : \frac{\partial \boldsymbol{m}}{\partial \boldsymbol{\sigma}} & \Delta\lambda \mathbf{C} : \frac{\partial \boldsymbol{m}}{\partial \boldsymbol{\kappa}} & \mathbf{C} : \boldsymbol{m} \\ -\frac{\partial \mathbf{A}}{\partial \boldsymbol{\sigma}} & \mathbf{I}^{sym} - \frac{\partial \mathbf{A}}{\partial \boldsymbol{\kappa}} & -\frac{\partial \mathbf{A}}{\partial \Delta\lambda} \\ \frac{\partial \phi}{\partial \boldsymbol{\sigma}} & \frac{\partial \phi}{\partial \boldsymbol{\kappa}} & 0 \end{array} \right]^{-1} \left[ \begin{array}{c} \mathbf{C} \\ \mathbf{0} \\ \mathbf{0} \end{array} \right]. \tag{3.10}$$

The consistent tangent operator $\frac{\partial \sigma}{\partial \boldsymbol{\Delta\varepsilon}}$ for CPPM can be found by solving the above at the converged state variables.

### 3.3 Proposed Method

As explained above, CPPM treats $\boldsymbol{\sigma}$, $\boldsymbol{\kappa}$ and $\Delta\lambda$ as independent variables, while CPM treats only $\Delta\lambda$ as the independent variable. Both the methods express $\phi$ as a function of the corresponding independent state variables at the $(k+1)^{th}$ iteration, which are unknown. To solve the resulting nonlinear equations, both the methods linearize sufficient number of fundamental expressions. CPPM consisting of several independent variables, obtains three sets of linear equations by linearizing the residues $\boldsymbol{r_\sigma}$ and $\boldsymbol{r_\kappa}$ given by Eq. 3.7 and $\phi$, about $\boldsymbol{\sigma}^k$, $\boldsymbol{\kappa}^k$. On the other hand, since CPM has only one variable, $\Delta\lambda$, linearization of only $\phi$ about $\boldsymbol{\sigma}^k$, $\boldsymbol{\kappa}^k$ produces sufficient number of equations. CPM is known to be less stable, compared to the unconditionally stable CPPM. While CPM uses a single constraint (equation) in the stress integration, the proposed method imposes equal number of constraints to that of CPPM on the state variables and the yield criterion by way of evaluating $\frac{\partial \sigma}{\partial \Delta\lambda}$ and $\frac{\partial \kappa}{\partial \Delta\lambda}$ of Eq. 3.2 at the unknown $(k+1)^{th}$ state, in addition to $\frac{\partial \phi}{\partial \Delta\lambda}$, thereby increasing the number of quantities evaluated at the unknown $(k+1)^{th}$ state to that of CPM.

The proposed algorithm relies on the fact that the rates of stress ($\dot{\boldsymbol{\sigma}}$), back stress ($\dot{\boldsymbol{\alpha}}$) and plastic strain ($\dot{\varepsilon}^p$ ) can be expressed as a function of $\dot{\lambda}$ during plastic deformation. Expressing $\dot{\boldsymbol{\sigma}}$, $\dot{\boldsymbol{\alpha}}$ and $\dot{\varepsilon}^p$as a function of $\dot{\lambda}$, we can obtain the following incremental forms of Eqs. (2.3), and (2.4).

$$
\begin{aligned}
\boldsymbol{\sigma}^{k+1} &= \begin{cases} \boldsymbol{\sigma}_e = \boldsymbol{\sigma}_n + \mathbf{C} : \boldsymbol{\Delta\varepsilon} & \text{if } k = 0 \\ \boldsymbol{\sigma}^k - \Delta\lambda \mathbf{C} : \boldsymbol{m}^{k+1} & \text{if } k > 0 \end{cases} \\
\boldsymbol{\kappa}^{k+1} &= \begin{cases} \boldsymbol{\kappa}_n & \text{if } k = 0 \\ \boldsymbol{\kappa}^k + \mathbf{A}\left(\boldsymbol{\sigma}^{k+1}(\Delta\lambda), \boldsymbol{\kappa}^{k+1}(\Delta\lambda)\right) & \text{if } k > 0 \end{cases}
\end{aligned} \tag{3.11}
$$

Using Taylor expansion, we obtain a first order approximation about the current state, $(.)^k$ for the yield function $\phi\left(\boldsymbol{\sigma}^{k+1}(\Delta\lambda), \boldsymbol{\kappa}^{k+1}(\Delta\lambda)\right) = 0$ as

$$
\begin{aligned}
\phi^{k+1} &\approx \phi^k + \frac{\partial \phi}{\partial \Delta\lambda}\delta\lambda \\
0 &= \phi^k + \left( \left.\frac{\partial \phi}{\partial \boldsymbol{\sigma}}\right|^k : \frac{\partial \boldsymbol{\sigma}}{\partial \Delta\lambda} + \left.\frac{\partial \phi}{\partial \boldsymbol{\kappa}}\right|^k : \frac{\partial \boldsymbol{\kappa}}{\partial \Delta\lambda} \right) \delta\lambda.
\end{aligned} \tag{3.12}
$$

The above expression for $\frac{\partial \phi}{\partial \Delta\lambda}$ and the partial differentiation of Eqs. (3.11) and (3.12) with respect to $\Delta\lambda$ provide the following linear set of equations which can be solved for the unknowns $\frac{\partial \boldsymbol{\sigma}}{\partial \Delta\lambda}$, $\frac{\partial \boldsymbol{\kappa}}{\partial \Delta\lambda}$ and $\frac{\partial \phi}{\partial \Delta\lambda}$.

$$
\begin{bmatrix} \frac{\partial \boldsymbol{\sigma}}{\partial \Delta\lambda} \\ \frac{\partial \boldsymbol{\kappa}}{\partial \Delta\lambda} \\ \frac{\partial \phi}{\partial \Delta\lambda} \end{bmatrix} = \begin{bmatrix} \mathbf{I}^{sym} + \Delta\lambda \mathbf{C} : \frac{\partial \boldsymbol{m}}{\partial \boldsymbol{\sigma}} & \Delta\lambda \mathbf{C} : \frac{\partial \boldsymbol{m}}{\partial \boldsymbol{\kappa}} & 0 \\ -\frac{\partial \mathbf{A}}{\partial \boldsymbol{\sigma}} & \mathbf{I}^{sym} - \frac{\partial \mathbf{A}}{\partial \boldsymbol{\kappa}} & 0 \\ \frac{\partial \phi}{\partial \boldsymbol{\sigma}} & \frac{\partial \phi}{\partial \boldsymbol{\kappa}} & -1 \end{bmatrix}^{-1} \begin{bmatrix} -\mathbf{C} : \boldsymbol{m} \\ \frac{\partial \mathbf{A}}{\partial \Delta\lambda} \\ 0 \end{bmatrix} \tag{3.13}
$$

$$
\delta\lambda = -\left(\frac{\partial \phi}{\partial \Delta\lambda}\right)^{-1} \phi^k \tag{3.14}
$$

Once $\frac{\partial \phi}{\partial \Delta\lambda}$ is found, $\delta\lambda$ can be found using Eq. (3.14), and the state variables can be updated as

$$
\begin{aligned}
\boldsymbol{\sigma}^{k+1} &= \boldsymbol{\sigma}^k + \frac{\partial \boldsymbol{\sigma}}{\partial \Delta\lambda}\delta\lambda \\
\boldsymbol{\kappa}^{k+1} &= \boldsymbol{\kappa}^k + \frac{\partial \boldsymbol{\kappa}}{\partial \Delta\lambda}\delta\lambda \\
\Delta\lambda &= 0 + \delta\lambda = \delta\lambda,
\end{aligned} \tag{3.15}
$$

until suitable convergence criteria are met.

Comparison of Eqs. 3.8 and 3.13 shows that the components in their right hand sides are identical, except the CPPM's residuals. In that respect, each material-level iteration of CPPM and the proposed method requires identical computational effort. The properties of the last column and row of the Eq. (3.13) allow us to uncouple and solve the linear system as two independent systems for $\left\{ \frac{\partial \boldsymbol{\sigma}}{\partial \Delta\lambda} \quad \frac{\partial \boldsymbol{\kappa}}{\partial \Delta\lambda} \right\}^T$ and $\frac{\partial \phi}{\partial \Delta\lambda}$, which slightly reduces the computational effort compared to CPPM.

The novel proposed algorithm preserves the characteristics of CPM that it successively linearizes the yield function at the current state to first estimate plastic consistency parameter using the derivatives of the state variables with respect to the plastic consistency parameter and then update the state variables. A pseudo code for the proposed algorithm is given in Algorithm 1, and Fig. 3.1c depicts the updating of stress during the return mapping iterations of the proposed algorithm.

**Algorithm 1:** A pseudo code of the proposed algorithm. $\eta_{(.)}$ is a suitable small number to check the convergence of the quantity (.).

**input :** $\boldsymbol{\Delta\varepsilon}_{n+1}$

**output:** $\boldsymbol{\Delta\varepsilon}^e_{n+1}$: elastic portion of $\boldsymbol{\Delta\varepsilon}_{n+1}$

$\boldsymbol{\kappa}_{n+1}$: plastic internal variables

$\boldsymbol{\sigma}_{n+1}$: state of stress after $(n+1)^{th}$ global-iteration

$\left.\frac{\partial\boldsymbol{\sigma}}{\partial\boldsymbol{\Delta\varepsilon}}\right|_{n+1}$: consistent tangent operator

```
// Elastic predictor
```

$\boldsymbol{\Delta\varepsilon}^e_{n+1} = \boldsymbol{\Delta\varepsilon}_{n+1}; \quad \boldsymbol{\sigma}^0 = \boldsymbol{\sigma}_n + \mathbf{C} : \boldsymbol{\Delta\varepsilon}^e_{n+1}; \quad \boldsymbol{\kappa}^0 = \boldsymbol{\kappa}_n;$

**if** $(\phi(\boldsymbol{\sigma}^0, \boldsymbol{\kappa}^0) < 0)$ **then** `// Check whether yielded`

  $\boldsymbol{\sigma}_{n+1} = \boldsymbol{\sigma}^0; \quad \boldsymbol{\kappa}_{n+1} = \boldsymbol{\kappa}^0; \quad \boldsymbol{\Delta\varepsilon}^e_{n+1} = \boldsymbol{\Delta\varepsilon}_{n+1};$

  **return**;

**else**

  `// Initialize state variable for the iteration` $k = 1$

  $\frac{\partial\boldsymbol{\sigma}}{\partial\Delta\lambda} = -\mathbf{C} : \boldsymbol{m}^0; \qquad \frac{\partial\boldsymbol{\kappa}}{\partial\Delta\lambda} = \left.\frac{\partial\mathbf{A}}{\partial\Delta\lambda}\right|^0;$

  $\delta\lambda = \left( \left.\frac{\partial\phi}{\partial\boldsymbol{\sigma}}\right|^0 : \frac{\partial\boldsymbol{\sigma}}{\partial\Delta\lambda} - \left.\frac{\partial\phi}{\partial\boldsymbol{\kappa}}\right|^0 : \frac{\partial\mathbf{A}}{\partial\Delta\lambda} \right)^{-1} \phi(\boldsymbol{\sigma}^0, \boldsymbol{\kappa}^0);$

  $\boldsymbol{\sigma}^1 = \boldsymbol{\sigma}^0 + \frac{\partial\boldsymbol{\sigma}}{\partial\Delta\lambda}\delta\lambda; \quad \boldsymbol{\kappa}^1 = \boldsymbol{\kappa}^0 + \frac{\partial\boldsymbol{\kappa}}{\partial\Delta\lambda}\delta\lambda; \quad \Delta\lambda = 0 + \delta\lambda = \delta\lambda;$

  $k = 1;$

  `// Successively linearize` $\phi^{k+1} = \phi(\boldsymbol{\sigma}^{k+1}, \boldsymbol{\kappa}^{k+1})$ `and update the state variables`

  **do**

  $$\begin{bmatrix} \frac{\partial\boldsymbol{\sigma}}{\partial\Delta\lambda} \\ \frac{\partial\boldsymbol{\kappa}}{\partial\Delta\lambda} \end{bmatrix} = \begin{bmatrix} \mathbf{I}^{sym} + \Delta\lambda\mathbf{C} : \frac{\partial\boldsymbol{m}}{\partial\boldsymbol{\sigma}} & \Delta\lambda\mathbf{C} : \frac{\partial\boldsymbol{m}}{\partial\boldsymbol{\kappa}} \\ -\frac{\partial\mathbf{A}}{\partial\boldsymbol{\sigma}} & \mathbf{I}^{sym} - \frac{\partial\boldsymbol{A}}{\partial\boldsymbol{\kappa}} \end{bmatrix}^{-1} \begin{bmatrix} -\mathbf{C} : \boldsymbol{m} \\ \frac{\partial\mathbf{A}}{\partial\Delta\lambda} \end{bmatrix};$$

  $\delta\lambda = -\left( \left.\frac{\partial\phi}{\partial\boldsymbol{\sigma}}\right|^k : \frac{\partial\boldsymbol{\sigma}}{\partial\Delta\lambda} + \left.\frac{\partial\phi}{\partial\boldsymbol{\kappa}}\right|^k : \frac{\partial\boldsymbol{\kappa}}{\partial\Delta\lambda} \right)^{-1} \phi^k;$

  `// Update the state variables`

  $\boldsymbol{\sigma}^{k+1} = \boldsymbol{\sigma}^k + \delta\boldsymbol{\sigma}$; where $\delta\boldsymbol{\sigma} = \frac{\partial\boldsymbol{\sigma}}{\partial\Delta\lambda}\delta\lambda$;

  $\boldsymbol{\kappa}^{k+1} = \boldsymbol{\kappa}^k + \delta\boldsymbol{\kappa}$; where $\delta\boldsymbol{\kappa} = \frac{\partial\boldsymbol{\kappa}}{\partial\Delta\lambda}\delta\lambda$;

  $\Delta\lambda = \delta\lambda;$

  $k = k + 1;$ `// increment the iteration index`

  **while** $\left(\left(\phi^k \leq \eta_\phi\right)\right.$ **or** $(\delta\boldsymbol{\sigma} < \eta_{\boldsymbol{\sigma}})$ **or** $\left.(\delta\boldsymbol{\kappa} < \eta_{\boldsymbol{\kappa}})\right)$

  $\boldsymbol{\sigma}_{n+1} = \boldsymbol{\sigma}^k; \quad \boldsymbol{\kappa}_{n+1} = \boldsymbol{\kappa}^k;$

  **return**;

Consistent Tangent Operator

By differentiating the set of equations given in Eq. (3.11) and the yield criterion with respect to $\boldsymbol{\Delta\varepsilon}$, we can obtain,

$$\begin{bmatrix} \left.\frac{\partial \sigma}{\partial \boldsymbol{\Delta\varepsilon}}\right|^{k+1} \\ \left.\frac{\partial \kappa}{\partial \boldsymbol{\Delta\varepsilon}}\right|^{k+1} \\ \left.\frac{\partial \Delta\lambda}{\partial \boldsymbol{\Delta\varepsilon}}\right|^{k+1} \end{bmatrix} = \begin{bmatrix} \mathbf{I}^{sym} + \Delta\lambda \mathbf{C} : \frac{\partial \boldsymbol{m}}{\partial \sigma} & \Delta\lambda \mathbf{C} : \frac{\partial \boldsymbol{m}}{\partial \kappa} & \mathbf{C} : \boldsymbol{m} \\ -\frac{\partial \mathbf{A}}{\partial \sigma} & \mathbf{I}^{sym} - \frac{\partial \boldsymbol{A}}{\partial \kappa} & -\frac{\partial \mathbf{A}}{\partial \Delta\lambda} \\ \frac{\partial \phi}{\partial \sigma} & \frac{\partial \phi}{\partial \kappa} & 0 \end{bmatrix}^{-1} \begin{bmatrix} \left.\frac{\partial \sigma}{\partial \boldsymbol{\Delta\varepsilon}}\right|^{k} \\ \left.\frac{\partial \kappa}{\partial \boldsymbol{\Delta\varepsilon}}\right|^{k} \\ \mathbf{0} \end{bmatrix} \tag{3.16}$$

The components of the inverted matrix in the right hand side are also evaluated using the state variables obtained at the end of the $(k+1)^{th}$iteration (i.e., the latest completed material-level iteration). The above recursive relation is repeatedly applied at the end of each material-level iteration, and the $\frac{\partial \sigma}{\partial \boldsymbol{\Delta\varepsilon}}$ obtained at the end of converged material-level iteration is the consistent tangent operator of the proposed algorithm.

While CPPM requires solving Eq. (3.10) only once at end of converged material-level iterations, the proposed requires recursively solving Eq. (3.16) at the end of each material-level iteration. This extra amount of computational effort is one major disadvantage of the proposed method compared to CPPM. As it will be demonstrated in the next section, both the CPPM and the proposed methods require the same number of global-level iterations indicating that the consistent tangent operators of both the methods perform equally.

### *3.4 Comparison of the Proposed Algorithm with CPPM and CPM*

From the formulation of the proposed integration scheme, we can establish the main features of the proposed integration scheme as,

- All three stress integration algorithms are implicit in the sense that in all three algorithms the unknown variables are evaluated at the unknown state.
- Uses satisfaction of implicit constitutive relations (Eq. (3.11) and $\phi^{k+1} = 0$) to arrive at an estimate for the plastic consistency parameter in contrast to the residual based approach used in CPPM. Successive linearization of the yield function around the current state is used to estimate the plastic consistency parameter using the derivatives of the state variables with respect to the plastic consistency parameter.
- Unlike in CPPM, the plastic consistency parameter is not continuously updated in the proposed method. Like in CPM, the plastic consistency parameter is found at each iteration separately and is not carried to the next iteration by additive updates.
- Like in CPPM, the first and second order derivatives of the yield surface and the plastic potential surface are used during the stress integration whereas in CPM only the first order derivatives are used.
- A consistent tangent operator is available for global iterations which has to be updated iteratively unlike in CPPM where the consistent tangent operator is evaluated explicitly at the end of successful convergence of the state variables. Therefore, the evaluation of the consistent tangent operator in the proposed method at the end of each material level iteration adds additional computational cost in comparison to CPPM.

It is evident that there are key distinguishable features that separate the proposed integration scheme from the veteran CPPM and CPM integration schemes. Further investigations are necessary to establish the numerical stability and usability of the proposed scheme for generalized plasticity models. In this paper, we consider the application of the proposed integration scheme for limited use in the von Misses model.

## 4 Verification tests

In this section, the accuracy and convergence behaviour of the algorithm is assessed and compared against CPPM and CPM, with two tests conducted using von Mises yield criterion. The following form of the von Mises yield function is used in all of the numerical simulations presented in this section. Note that the Frobenius norm ($\|.\|_{\mathcal{F}}$) of a second order arbitrary tensor, $\mathbf{A}$, is $\|\mathbf{A}\|_{\mathcal{F}} = \sqrt{\mathbf{A} : \mathbf{A}}$.

$$\phi = \sqrt{\frac{3}{2}}\,\|\boldsymbol{s} - \boldsymbol{\alpha}\|_{\mathcal{F}} - (\sigma_{y,0} + A_I e^p) \tag{4.1}$$

Here, $\boldsymbol{\alpha}$ is the back stress defined by Eq. (4.2) following Ziegler's rule [11, 12],

$$\dot{\boldsymbol{\alpha}} = A_k\left(\boldsymbol{\sigma}, \boldsymbol{\alpha}\right)\dot{e}^p\left(\boldsymbol{\sigma} - \boldsymbol{\alpha}\right) \tag{4.2}$$

$A_K$,$\sigma_{y,0}$, and $A_I$ are kinematic hardening modulus (constant), initial yield stress, and isotropic hardening modulus (constant). By virtue of setting different values for $A_K$ and $A_I$, linear kinematic hardening ($A_I = 0$), linear isotropic hardening ($A_K = 0$), and combined hardening ($A_I, A_K \neq 0$) phenomena could be simulated. $e^p$ is the effective plastic strain which is a stress integration algorithm dependent quantity and is defined as follows (here, $\boldsymbol{e}^p$ is the deviatoric part of plastic strain),

$$e^p = \int_0^t \sqrt{\frac{2}{3}}\,\|\dot{\boldsymbol{e}}^p\|_{\mathcal{F}}\,dt \tag{4.3}$$

For the proposed integration method, it follows from the incremental form representation of plastic strain, $\boldsymbol{\varepsilon}^{p,k+1} = \boldsymbol{\varepsilon}^p + \Delta\lambda\boldsymbol{m}^{k+1}$, that (Here, $\boldsymbol{d}$ is the deviatoric part of $\boldsymbol{m}$),

$$e^{p,k+1} = \begin{cases} e^p_n & \text{if } k = 0 \\ e^p_n + \sqrt{\frac{2}{3}}\left\|\boldsymbol{e}^{p,k} + \Delta\lambda\boldsymbol{d}^{k+1}\right\|_{\mathcal{F}} & \text{if } k > 0 \end{cases} \tag{4.4}$$

Furthermore, we use the following incremental forms for back stress in each of the stress integration methods considered,

$$\boldsymbol{\alpha}^{k+1} = \begin{cases} \boldsymbol{\alpha}_n & \text{if } k = 0 \\ \boldsymbol{\alpha}^k + \frac{\Delta\lambda A_K}{\sigma_e}\sqrt{\frac{2}{3}}\left\|\boldsymbol{d}^k\right\|_{\mathcal{F}}\mathbf{P}^{sd} : \left(\boldsymbol{\sigma}^k - \boldsymbol{\alpha}^k\right) & \text{if } k > 0, \end{cases} \qquad \text{CPM} \tag{4.5}$$

$$\boldsymbol{\alpha}^{k+1} = \begin{cases} \boldsymbol{\alpha}_n & \text{if } k = 0 \\ \boldsymbol{\alpha}^k + \frac{\Delta\lambda^{k+1} A_K}{\sigma_e}\sqrt{\frac{2}{3}}\left\|\boldsymbol{d}^{k+1}\right\|_{\mathcal{F}}\mathbf{P}^{sd} : \left(\boldsymbol{\sigma}^{k+1} - \boldsymbol{\alpha}^{k+1}\right) & \text{if } k > 0, \end{cases} \qquad \text{CPPM} \tag{4.6}$$

$$\boldsymbol{\alpha}^{k+1} = \begin{cases} \boldsymbol{\alpha}_n & \text{if } k = 0 \\ \frac{A_K}{\sigma_e}\sqrt{\frac{2}{3}}\left\|\boldsymbol{e}^{p,k} + \Delta\lambda\boldsymbol{d}^{k+1}\right\|_{\mathcal{F}}\mathbf{P}^{sd} : \left(\boldsymbol{\sigma}^{k+1} - \boldsymbol{\alpha}^{k+1}\right) & \text{if } k > 0, \end{cases} \qquad \text{Proposed} \tag{4.7}$$

Here, $\mathbf{P}^{sd} = \mathbf{I}^{sym} - \frac{1}{3}\mathbf{I} \otimes \mathbf{I}$ is the fourth order isotropic tensor that converts any second-order tensor into its symmetric-deviator form [13] and $\sigma_e = \sqrt{\frac{3}{2}}\, \|\boldsymbol{s} - \boldsymbol{\alpha}\|_{\mathcal{F}}$.

Numerical tests are conducted for the following cases,

1. Single material point.
2. Uniaxial extension of a perforated sheet.

using all three stress integration algorithms CPPM, CPM, and the proposed method. The algorithms were implemented in C++ with the matrix operations undertaken using the Eigen library[14], a software library written in C++ for matrix computations.

### *4.1 Single material point*

The accuracy of the proposed method is demonstrated using the semi-analytical solutions provided in Anandarajah [4] and Kim [15] for two problems, i.e., linear isotropic hardening and combined hardening respectively. The two sets of material parameters used in the respective problems are (Here, $E$ is the modulus of elasticity and $\nu$ is the Poisson's ratio),

1. Material 1: $E = 200$ GPa; $\nu = 0.3$; $A_I = 20$ GPa; $A_K = 0$ MPa; $\sigma_{y,n} = 0.25$ GPa
2. Material 2: $E = 2.4$ GPa; $\nu = 0.2$; $A_I = 70$ MPa; $A_K = 30$ MPa; $\sigma_{y,n} = 300$ MPa

For the linear isotropic hardening problem in Anandarajah [4] with the initial state, $\boldsymbol{\sigma}_n = \left\{ \begin{array}{cccccc} 0.1 & 0.05 & 0.075 & 0 & 0 & 0 \end{array} \right\}^{\mathrm{T}}$ GPa and the applied strain increment, $\boldsymbol{\Delta\varepsilon} = \left\{ \begin{array}{cccccc} 0.03 & -0.028 & 0.01 & 0 & 0 & 0 \end{array} \right\}^{\mathrm{T}}$, Table 1 provides the remapped stresses obtained from the three numerical integration schemes of interest. The results are compared against the semi-analytical solution provided in Anandarajah [4] and the converged results obtained using CPPM by applying subincrements (using 1024 subincrements of the strain increment). The relative error in Table 1, $E_R$, defined by,

$$E_R = \frac{\|\boldsymbol{\sigma}_{num} - \boldsymbol{\sigma}_{ref}\|}{\|\boldsymbol{\sigma}_{ref}\|} \tag{4.8}$$

where $\boldsymbol{\sigma}_{num}$ is the numerical integration result from the numerical integration without any subincrementation and $\boldsymbol{\sigma}_{ref}$ is the reference converged result obtained by applying CPPM using subincrementation [16]. From the results, it is clear that no significant disparity exists between the numerical integration results obtained from all three numerical integration schemes. Furthermore, all stress integration algorithms took only a single material point iteration to produce the following set of remapped results.

**Table 1: Remapped stresses comparison - Linear Isotropic Hardening (Units are in GPa)**

| Stress | Integration Scheme | | | | |
|---|---|---|---|---|---|
| components | Semi-Analytical | Subincrements | CPPM | CPM | Proposed |
| $\sigma_{11}$ | 2.51333 | 2.51297 | 2.51333 | 2.51333 | 2.51333 |
| $\sigma_{22}$ | 1.53615 | 1.53596 | 1.53615 | 1.53615 | 1.53615 |
| $\sigma_{33}$ | 2.17552 | 2.17607 | 2.17552 | 2.17552 | 2.17552 |
| $\sigma_{12}$ | 0 | 0 | 0 | 0 | 0 |
| $\sigma_{13}$ | 0 | 0 | 0 | 0 | 0 |
| $\sigma_{23}$ | 0 | 0 | 0 | 0 | 0 |
| $E_R$ | 0.000185 | - | 0.000185 | 0.000185 | 0.000185 |

Kim [13] provides a combined hardening problem with $\boldsymbol{\sigma}_n = \left\{ \begin{array}{cccccc} 300 & 0 & 0 & 0 & 0 & 0 \end{array} \right\}^{\mathrm{T}}$ MPa as the initial state and the applied strain increment, $\boldsymbol{\Delta\varepsilon} = \left\{ \begin{array}{cccccc} 0.1 & -0.02 & -0.02 & 0 & 0 & 0 \end{array} \right\}^{\mathrm{T}}$. Table 2 shows the remapped stresses obtained from the three stress integration algorithms in relation to the semi-analytical solution provided in Kim [13] and the converged results obtained using CPPM by applying subincrements (using 1024 subincrements of the strain increment). From the results, it is evident that all three stress integration algorithms provide identical estimates for the remapped stresses. As in the previous case, here also only a single material point iteration was utilized by each of the stress integration algorithms to produce the following remapped stresses.

**Table 2: Remapped stresses comparison - Combined Hardening (Units are in MPa)**

| Stress | Integration Scheme | | | | |
|---|---|---|---|---|---|
| components | Semi-Analytical | Subincrements | CPPM | CPM | Proposed |
| $\sigma_{11}$ | 385.16129 | 385.16129 | 386.65972 | 386.65972 | 386.65972 |
| $\sigma_{22}$ | 77.41935 | 77.41935 | 76.67013 | 76.67013 | 76.67013 |
| $\sigma_{33}$ | 77.41935 | 77.41935 | 76.67013 | 76.67013 | 76.67013 |
| $\sigma_{12}$ | 0 | 0 | 0 | 0 | 0 |
| $\sigma_{13}$ | 0 | 0 | 0 | 0 | 0 |
| $\sigma_{23}$ | 0 | 0 | 0 | 0 | 0 |
| $E_R$ | $3.37 \times 10^{-14}$ | - | 0.004583 | 0.004583 | 0.004583 |

### *4.2 Uniaxial extension of a perforated sheet*

The overall performance of the proposed integration scheme (specifically the consistent tangent operator) is evaluated and compared with CPPM and CPM (with continuum tangent operator) on an elastoplastic homogeneous thin square shaped perforated sheet. The square sheet measures 20 mm a side, a thickness of 1 mm with a central circular hole of radius 1 mm. Considering the symmetry of the sheet, we model only a quarter of the sheet with the appropriate symmetric boundary conditions (Fig. 4.1a). A structured mesh with $1024 \times 3$ 8-node brick elements and 4356 nodes is used.

The sheet is subjected to a uniform distributed load of magnitude 400 $\mathrm{N/mm^2}$ applied perpendicular to the top edge as shown in Fig. 4.1a according to the cyclic loading history given in

Fig. 4.1b using load control. The total analysis time is 4.0 s with time step increments ($\Delta t$) of 0.1 s corresponding to 40 steps. We consider three three-dimensional problems using the same mesh and boundary conditions, i.e., linear isotropic hardening, linear kinematic hardening, and linear combined hardening. The set of material parameters used in the respective problems are as follows,

1. Material 3: $E = 206.9$ GPa; $\nu = 0.29$; $A_I = 10000$ MPa; $A_K = 0$ MPa; $\sigma_{y,0} = 450$ MPa
2. Material 4: $E = 206.9$ GPa; $\nu = 0.29$; $A_I = 0$ MPa; $A_K = 10000$ MPa; $\sigma_{y,0} = 450$ MPa
3. Material 5: $E = 206.9$ GPa; $\nu = 0.29$; $A_I = 5000$ MPa; $A_K = 5000$ MPa; $\sigma_{y,0} = 450$ MPa

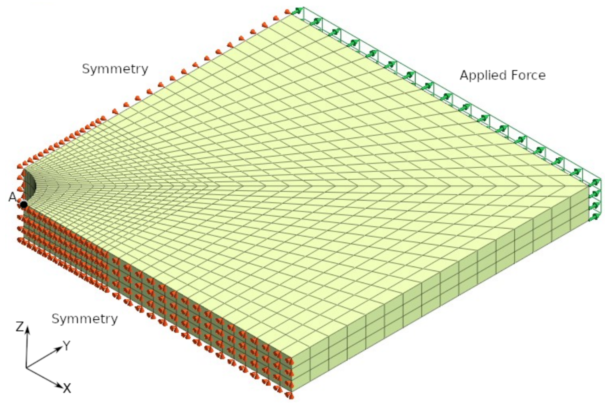


(a) Mesh and boundary conditions

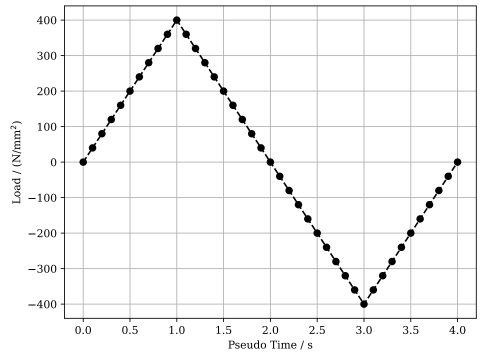


(b) Cyclic loading history Vs pseudo time

**Figure 4.1: Three-dimensional perforated sheet.**

We compare the three methods using the displacement measured at node A along the X - axis direction($u_x$) during the loading and unloading cycles. We define time-step-wise percentage deviation ($E_{r,dev\%}$) metric as follows, which is used to illustrate the accuracy of a certain algorithm with respect to the results from another reference stress integration algorithm.

$$E_{r,dev\%} = \frac{|d_{method} - d_{ref}|}{|d_{ref}|_{max}} \times 100\% \tag{4.9}$$

Here, $d_{method}$ is the displacement at a particular node obtained using the "method" (method could be CPM, CPPM or Proposed) stress integration algorithm at a particular pseudo time step where as $d_{ref}$ is the displacement at the same node obtained using the reference method of stress integration at a particular pseudo time step. $|d_{ref}|_{max}$ refers to the maximum absolute value of displacement recorded at the same node obtained using the reference method from all the time steps. All three stress integration implementations use the same convergence criteria for global iterations and the local material point iterations.

### 4.2.1 Linear Isotropic Hardening and Linear Kinematic Hardening

Fig. 4.2a and Fig.4.3a depict the displacement vs load increment for linear isotropic hardening and linear kinematic hardening conducted using material 3 and material 4 set parameters respectively. All three stress integration methods give near identical results for both linear isotropic hardening and linear kinematic hardening cases. This is evident from Fig. 4.2b and Fig. 4.3b which show the percentage deviation with respect to results from CPPM for linear isotropic hardening and linear kinematic hardening respectively. Fig. 4.2c and Fig.4.3c depict the number of iterations taken by each of the stress integration algorithms during global iterations for linear isotropic hardening and linear kinematic hardening respectively. As you can see, the the proposed scheme and CPPM have consumed the same number of global iterations (102 iterations) for linear isotropic hardening case. For linear kinematic hardening case both the proposed scheme and CPPM have utilized the same number of global iterations (136 iterations). The CPM takes a considerably large number of global iterations for linear isotropic hardening case (256 iterations) as well as for linear kinematic hardening case (351 iterations) to give the same comparable results.

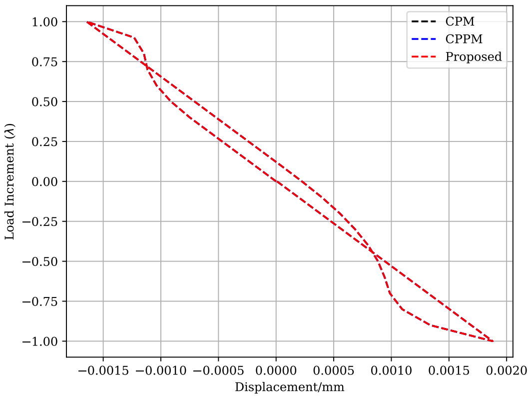


(a) Displacement vs load increment

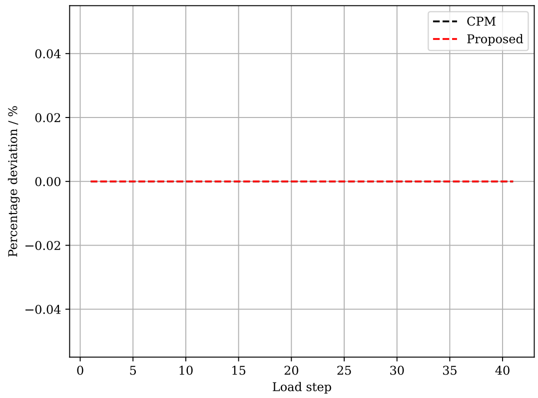


(b) Percentage deviation with respect to results from CPPM ($\Delta t = 0.1s$)

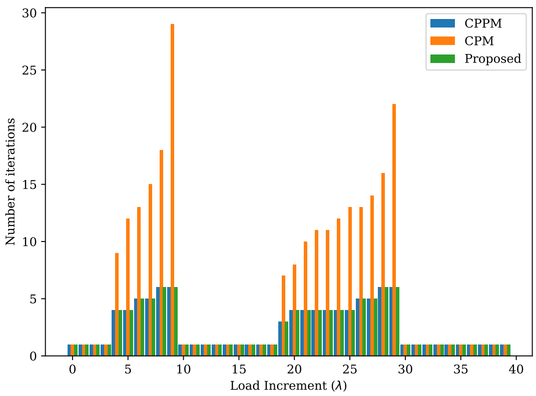


(c) Number of iterations taken by each algorithm at global-level

**Figure 4.2: Perforated sheet - Isotropic hardening**

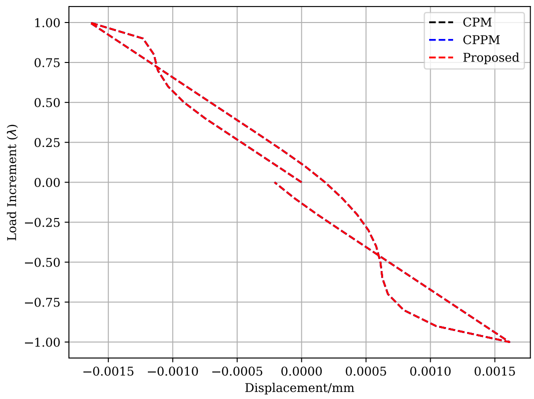


(a) Displacement vs load increment

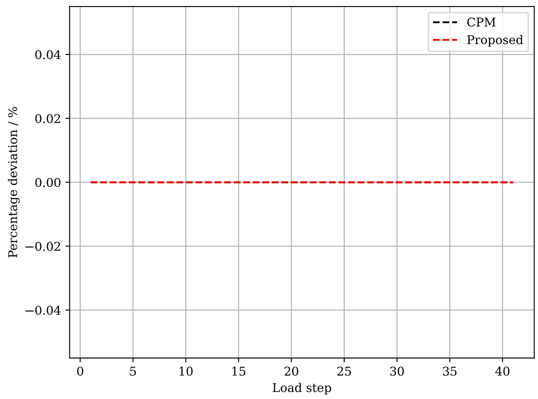


(b) Percentage deviation with respect to results from CPPM ($\Delta t = 0.1s$)

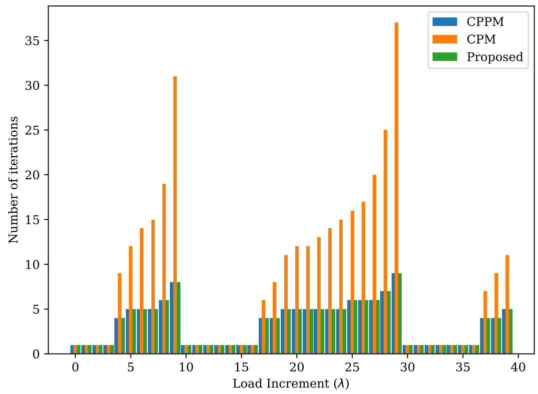


(c) Number of iterations taken by each algorithm at global-level

**Figure 4.3: Perforated sheet - Kinematic hardening**

### 4.2.2 Combined Hardening

The displacement vs load increment variation for combined hardening conducted using material 5 set parameters is shown in Fig. 4.4a. Here, we can observe that CPM and the proposed method follow near identical trajectories where as CPPM exhibits a significantly different trajectory after the 19$^{\text{th}}$load step. This is evident from Fig. 4.4b which shows the percentage deviation with respect to results from CPPM. Fig. 4.4c exhibits the number of iterations taken by each of the stress integration algorithms during global iterations. Here, we can observe that the the proposed scheme and CPPM record the same number of global iterations (116 iterations) where as CPM consumes a considerably large number of global iterations (287 iterations) to give the same comparable results.

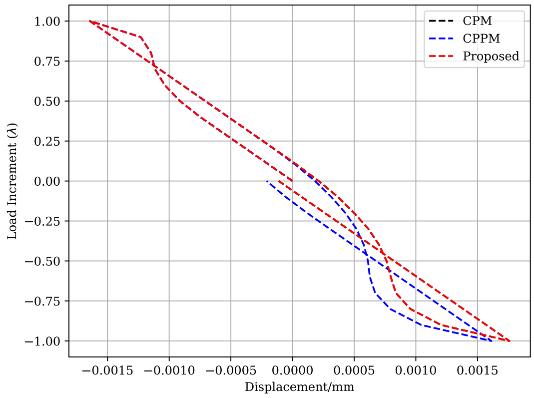


(a) Displacement vs load increment

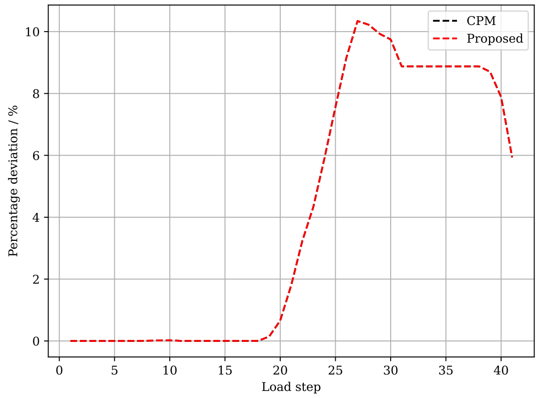


(b) Percentage deviation with respect to results from CPPM ($\Delta t = 0.1s$)

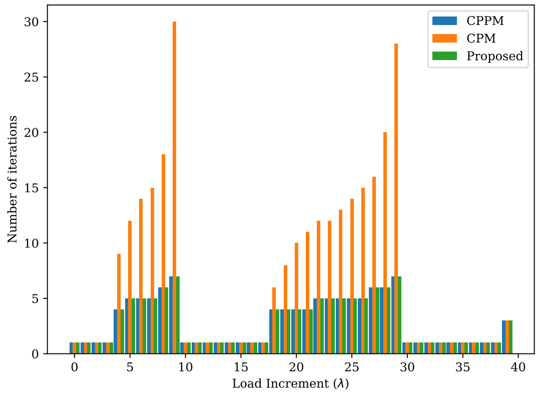


(c) Number of iterations taken by each algorithm at global-level

**Figure 4.4: Perforated sheet - Combined hardening**

## 5 Summary and Concluding Remarks

In this paper, a novel implicit stress integration algorithm which consists of some of the properties of CPPM and CPM is presented. In fact, the first and second order derivatives in the proposed stress are the same as that of CPPM (see Eq. (3.7) and Eq. (3.13)). The proposed implicit algorithm, uses satisfaction of implicit constitutive relations and successive linearization of the yield function around the current state to arrive at an estimate for the plastic consistency parameter required to update the state variables, in contrast to to the residual based approach used in CPPM. The successive linearization of the yield function about the current state to evaluate the state variables is a feature that the proposed stress integration scheme shares with CPM. However, the proposed method imposes equal number of constraints (equations) to that of CPPM by way of evaluating the derivatives of the state variables and the yield criterion with respect to the plastic consistency parameter in contrast to the single constraint (equation) used by CPM in the stress integration procedure. Further, unlike in CPM, it is straightforward to derive a consistent tangent operator for the proposed method.

Several verification tests are performed using the von Mises yield criterion to verify the proposed stress integration scheme and compare its performance in relation to CPPM and CPM. Single material point tests are performed to verify the accuracy of the stress integration procedure whereas the multi-element tests are carried out to verify and evaluate the performance of the consistent tangent operator. In the context of von Misses model for material point iterations, the following can be inferred,

- the stress integration results of the proposed algorithm are on par with the results from CPPM and CPM for linear hardening rules.
- the computational cost associated with material point iterations (per iteration basis, when evaluation of the consistent tangent operator is excluded) is lowest for CPM and highest for CPPM where as the computational cost of the proposed scheme is marginally less than CPPM. Since, only first order derivatives are required for CPM, it has the lowest computational cost. In the proposed scheme the number of linear simultaneous equations that need to be solved per iteration is always one less than the number of linear simultaneous equations that need to be solved for CPPM. This reduces the computational cost of the proposed scheme marginally in comparison to CPPM.

In the context of von Misses model for global level iterations for linear hardening rules, the following can be inferred,

- the accuracy of the global response results are on par with CPPM with the consistent tangent operator and CPM with the continuum tangent operator.
- identical number of global level iterations to that of CPPM are required to obtain the converged solutions. This implies that the consistent tangent operator obtained form the proposed scheme is as good as the CPPM counterpart. CPM reporting the highest number of global level iterations could be attributed to using the continuum tangent operator.
- the total computational cost per material point evaluation which includes the cost associated with the stress integration as well as the consistent tangent operator evaluation, is lowest for CPM and highest for the proposed scheme due to the iterative nature of the consistent tangent operator of the proposed scheme. However, this disadvantage of solving for the small (at most $13\times13$ for isotropic material) consistent tangent operator several times during a material point iteration dwarfs in comparison to the advantage yielded through the use of a consistent tangent operater at the global iterations due to second order convergence.

From the results, it is evident that the proposed scheme is a viable alternative for elastoplastic stress integration of von Mises plasticity as it provides comparable results to that of CPPM and CPM. As the first and second order derivatives required in the stress integration procedure of the proposed method are the same as that of CPPM, one can easily implement the proposed method in existing finite element analysis frameworks. In the future, we plan to explore proposed methods performance in simulating complex palsticty models like Drucker-Prager and Cam-Clay.

## Acknowledgments

This work was supported by JSPS Kakenhi grant 22H01573.

## References

[1] Scalet, G., Auricchio, F., (2018). Computational Methods for Elastoplasticity: An Overview of Conventional and Less-Conventional Approaches. *Arch Computat Methods Eng*, **25**, 545–589.

[2] Wilkins, M.L. (1964). Calculation of elasto-plastic flow. In Methods of Computational Physics 3, Academic, New York.

[3] Ortiz, M. and Simo, J.C. (1986). Analysis of a new class of integration algorithms for elastoplastic constitutive relations. *International Journal for Numerical Methods in Engineering*, **23**: 353–366.

[4] Anandarajah, A., (2010). Computational methods in elasticity and plasticity: solids and porous media. Springer, New York.

[5] Simo, J. C., and Hughes T. J. R., (1998), *Computational Inelasticity*, Springer, New York.

[6] Neto, E.A. de S., Perić, D., Owen, D.R.J., (2008). Computational methods for plasticity: theory and applications. Wiley, Chichester, West Sussex, UK.

[7] Coleman, B.D. (1964). Thermodynamics of materials with memory. *Archive for Rational Mechanics and Analysis*, **17**: 1.

[8] Starman, B., Halilovič, M., Vrh, M., Štok, B., (2014). Consistent tangent operator for cutting-plane algorithm of elasto-plasticity. *Comput. Methods Appl. Mech. Eng.*, **272**: 214–232.

[9] Krieg, R.D. and Krieg, D.B. (1977). Accuracies of numerical solution methods for the elastic perfectly plastic model. *Transactions of ASME Journal of Pressure Vessel Technology*, **99**: 510–515.

[10] Simo, J.C. and Taylor, R.L. (1985). Consistent tangent operators for rate-independent elastoplasticity. *Computer Methods in Applied Mechanics and Engineering*, **48**: 101–118.

[11] Shield, R. and Ziegler, H. (1958). On Prager's hardening rule. *Journal of Applied Mathematics and Physics (ZAMP)*, 9a: 260.

[12] Ziegler, H. (1959). A modification of Prager's hardening rule. *Quarterly of Applied Mathematics*, 17: 55.

[13] Pedroso, D.M., Sheng, D., Sloan, S.W. (2008). Stress update algorithm for elastoplastic models with nonconvex yield surfaces. *Int. J. Numer. Meth. Engng,* **76**, 2029–2062.

[14] Guennebaud, G., et al. (2010). Eigen V3. http://eigen.tuxfamily.org (Retrieved on 22 April, 2022).

[15] Kim, N. H. (2015). Introduction to Nonlinear Finite Element Analysis. Springer US, New York, NY.

[16] Dodds, R.H., (1987). Numerical techniques for plasticity computations in finite element analysis. *Computers & Structures*, **26**, 767–779.